

Article

# Modeling of Atmospheric Carbon Dioxide (CO<sub>2</sub>) Concentrations as a Function of Fossil-Fuel and Land-Use Change CO<sub>2</sub> Emissions Coupled with Oceanic and Terrestrial Sequestration

John P. O'Connor

Aqua-Solar Industries LLC, 4 Lamancha Way, Andover, MA 01810, USA; j9oconn@aol.com

Received: 20 February 2020; Accepted: 28 April 2020; Published: 2 May 2020

**Abstract:** In this work, a semi-empirical relationship of carbon dioxide emissions with atmospheric CO<sub>2</sub> concentrations has been developed that is capable of closely replicating observations from 1751 to 2018. The analysis was completed using data from fossil-fuel-based and land-use change based CO<sub>2</sub> emissions, both singly and together. Evaluation of emissions data from 1750 to 1890 yields a linear CO<sub>2</sub> concentration component that may be attributed to the net flux from land-use changes combined with a rapidly varying component of the terrestrial sink. This linear component is then coupled across the full-time period with a CO<sub>2</sub> concentration calculation using fossil-fuel combustion/cement production emissions with a single, fixed fossil-fuel combustion airborne fraction [AF<sub>FF</sub>] value that is determined by the ocean sink coupled with the remaining slowly varying component of the land sink. The analysis of the data shows that AF<sub>FF</sub> has remained constant at 51.3% over the past 268 years. However, considering the broad range of variables including emission and sink processes influencing the climate, it may not be expected that a single value for AF<sub>FF</sub> would accurately reproduce the measured changes in CO<sub>2</sub> concentrations during the industrial era.

**Keywords:** CO<sub>2</sub> emissions; CO<sub>2</sub> concentrations; atmospheric fraction

---

## 1. Introduction

In 1861, Irish physicist John Tyndall presented results from his measurements on the absorption of “calorific rays” by various gases to the Royal Society [1,2]. This presentation is believed to be the first attribution of atmospheric greenhouse gases, and specifically of water vapor and carbon dioxide, to changes in the climate. Since that time and especially for the past several decades, there has been a significant focus upon the emissions of CO<sub>2</sub> into the atmosphere and the potential impact of increasing atmospheric CO<sub>2</sub> concentrations upon the global climate (see, e.g., [3–5]).

Sources of anthropogenic carbon emissions include releases from fossil fuel consumption/combustion and cement production as well as from land-use changes. Fossil-fuel-driven emission data are collected and reported by a number of organizations [6–9] including the Carbon Dioxide Information Analysis Center [CDIAC], the International Energy Agency [IEA], the United Nations [UN], and the United States Department of Energy [DoE] Energy Information Administration [EIA]. Carbon emissions emanating from land-use change have been studied by, e.g., Stocker et al. [10] and Le Quéré et al. as part of the Global Carbon Budget [9].

Similar to Le Quéré et al. [9], the current investigation utilizes the CDIAC data set [7,8] of energy-based, human-caused carbon emissions since 1751. The data include total carbon emissions from fossil fuel consumption and cement production and are shown in Figure 1(a). Emissions have been increasing steadily for over 250 years and there has been a substantial increase in emissions since 1950 that has continued to the present [e.g., from 3 million metric tons in 1751 to 1,630 million tons in 1950 and increasing to 37,100 million tons in 2018] [7–9]. Uncertainties in the fossil fuel emission data have been estimated to range from 5% to 10% [9,11–13]. CO<sub>2</sub> emissions resulting from land-use changes are shown in Figure 1(b). The data demonstrate continually increasing CO<sub>2</sub> releases until approximately 1960. Slightly lower emission rates with increased variability have been observed since that time [9,10]. Land-use change emissions are estimated to include uncertainties of approximately 7% based on comparisons of the simulations used in Stocker [10] with Land-Use Harmonization approaches [14]. However, the Global Carbon Project [9] indicates uncertainties ranging from 31% to 53% at one sigma.

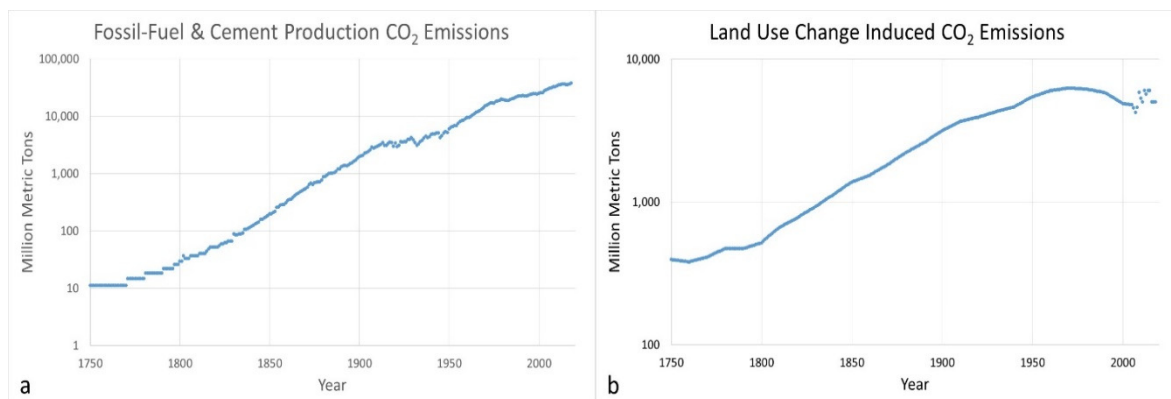


**Figure 1.** (a) Global CO<sub>2</sub> emissions into the environment from fossil fuel consumption and cement production [7,8], (b) global CO<sub>2</sub> emissions from land-use changes [9,10].

Figure 2 displays the measurements of the CO<sub>2</sub> concentration in the atmosphere based on the Law Dome [15] and Siple [16] ice cores and direct measurements at Mauna Loa [17,18]. The ice core data typically have temporal accuracy of  $\pm 2$  years while the CO<sub>2</sub> values for ice samples from within an annual layer were found to vary by less than 1.2 ppm [15]. For Mauna Loa, CO<sub>2</sub> concentrations are accurate to within  $\pm 0.2$  ppm [19]. These data demonstrate that the CO<sub>2</sub> concentration has been increasing steadily since 1750 and this increase has also accelerated significantly since 1960.

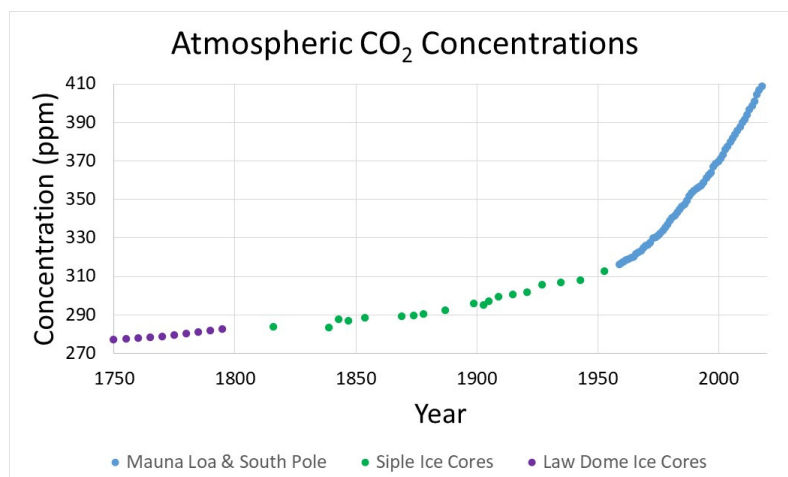


**Figure 2.** Observations of atmospheric CO<sub>2</sub> concentrations (ppm) [15–18]

Efforts to associate the change in CO<sub>2</sub> concentration with emissions based on a variety of models have been attempted. Many of these studies examined the uptake of CO<sub>2</sub> by the ocean as it is a large carbon sink in the environment. Examples include, study of the magnitude, variability, and trends in the global ocean carbon uptake [20], examination of feedback mechanisms and sensitivities of ocean carbon uptake under global warming [21], and reconstructions of the history of anthropogenic CO<sub>2</sub> concentrations in oceans [22]. These studies demonstrate that the CO<sub>2</sub> uptake by the ocean has been increasing over the past several decades and, at present, approximately 1 gram of CO<sub>2</sub> is absorbed by the ocean for every 4 grams emitted into the atmosphere [9].

With more than one-third of the earth's surface already altered by land-use changes (LUC) [23], it is important to consider both the past and future potential impacts of LUC on CO<sub>2</sub> concentrations and the climate. These impacts have been the subject of several studies [24–30]. LUC emissions have been estimated to increase CO<sub>2</sub> concentrations by 15–43 ppm during the time period of interest [24,25,28,29]. Bennedsen et al. [30] have performed statistical analyses to examine variations in the ocean and land sinks and the atmospheric fraction (AF). Their analysis yielded no statistical evidence that AF is varying but did find that the land sink rate was decreasing [30].

In this work, a simple semi-empirical parameterization has been developed to attempt to precisely reproduce the increase of atmospheric CO<sub>2</sub> concentrations observed from 1751 to 2018 resulting from increase in fossil fuel and land-use change emissions of CO<sub>2</sub> into the environment. Comparisons with observed CO<sub>2</sub> concentrations are presented. Implications of this analysis for the terrestrial sink and the determination of AF<sub>FF</sub> are discussed.

## 2. Materials and Methods

This work analyzed data sets containing CO<sub>2</sub> emissions from fossil fuel combustion [7–9] and land-use changes [9,10] to determine their impact upon CO<sub>2</sub> atmospheric concentrations. This assessment included:

- An evaluation of fossil fuel and land-use change CO<sub>2</sub> emissions with determination of best fit exponential or linear trendlines to enable comparison with prior studies, e.g., [31];
- The development of a semi-empirical model to calculate atmospheric CO<sub>2</sub> concentrations based on the level of fossil fuel and land-use emissions;
- To compare the model results of CO<sub>2</sub> concentration calculations using both
  - the traditional atmospheric fraction (AF), and,
  - a new approach that employs only AF<sub>FF</sub> combined with a linear component that addresses the net flux of land-based CO<sub>2</sub> emissions combined with a rapidly varying component of the terrestrial sink;
- To determine a value for AF<sub>FF</sub> for the time period under consideration.

## 3. Results

### 3.1. Correlation of Atmospheric CO<sub>2</sub> Concentration with CO<sub>2</sub> Emissions

#### 3.1.1. Traditional Approach and Discussion

The growth of carbon emissions from land-use changes [9,10,32] coupled with the burning of fossil fuels [7–9] is shown in Figure 3 [see Supplementary Material]. It is noted that an exponential growth curve will generally follow the overall shape of the observed data set, notwithstanding significant differences of up to 38% from the published data. It has been postulated that if the climate system is considered as a linear system forced by exponentially growing CO<sub>2</sub> emissions, then all ratios of responses to forcings are constant [31]. In particular, AF would be constant with the value dependent upon the lifetime,  $\tau$ , of the CO<sub>2</sub> in the atmosphere [33]. A best fit to the exponential emissions growth curve yields a value of approximately 43% for AF [33].

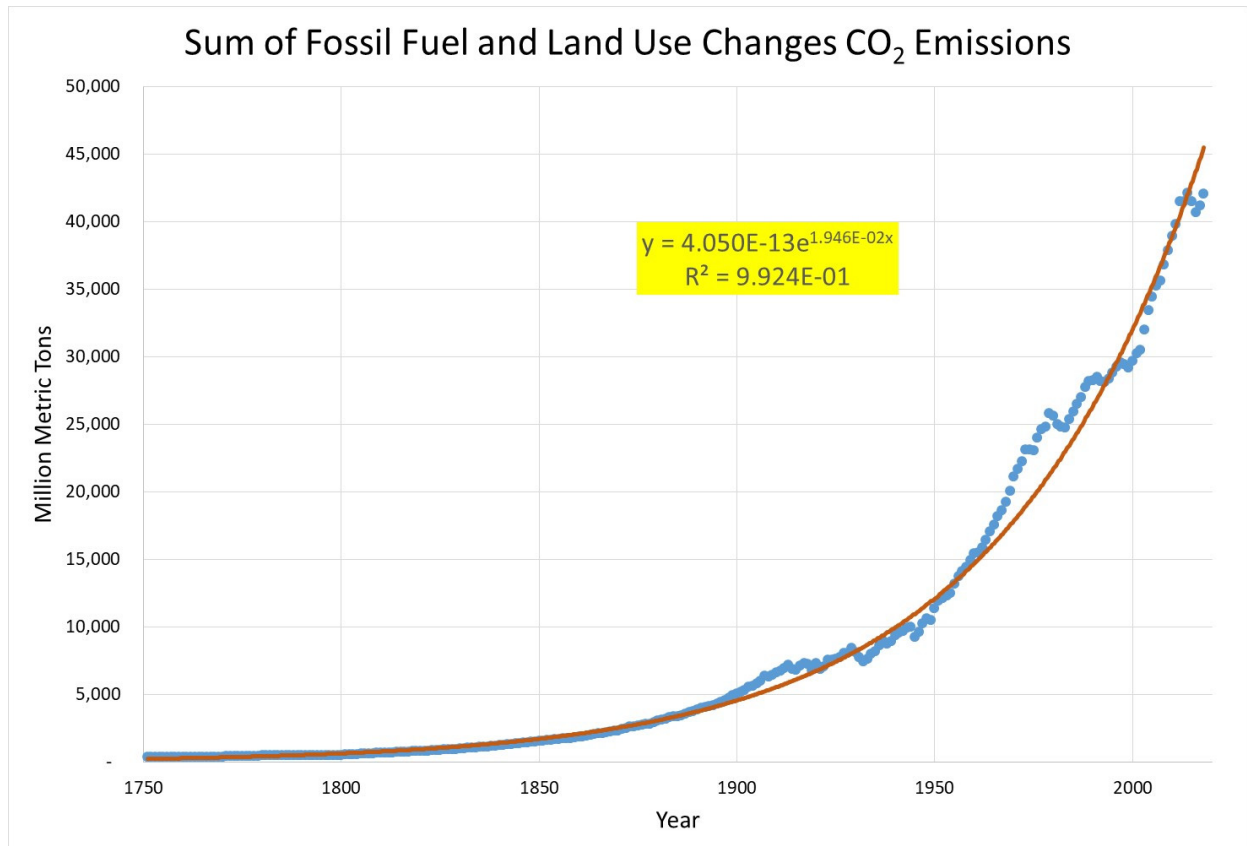


**Figure 3.** Global emission levels of CO<sub>2</sub> from fossil fuels and land-use changes; equation is best fit exponential curve to the data; R<sup>2</sup> in each figure defines the goodness of fit.

To convert the emissions data shown in Figure 3 to changes in atmospheric CO<sub>2</sub> concentrations, a measured base-year [2018] concentration datum of 408.52 ppm was chosen from the Mauna Loa CO<sub>2</sub> measurements data set [17,18]. The change in the atmospheric CO<sub>2</sub> concentration was then determined by using the combined fossil-fuel-based [7,8] and land-use changes induced CO<sub>2</sub> emissions [9,10] for each year preceding 2018, converting those annual emission rates into an equivalent ppm of the atmosphere [mass of the atmosphere = 5.148E18 kg [34]], and then applying a single scaling factor to determine the concentration change for that year. For each year prior to 2018, the change was negative. The governing equation is:

$$ATM_{N-1} = ATM_N - (\alpha_i/\beta) \times E_{N-1} \times 10^9 \quad (1)$$

where ATM is an atmospheric concentration in ppm,  $\alpha_i$  is the atmospheric fraction [ $\alpha_1$  determined by best fit to be 43.1%],  $\beta = 7.782Pg$  of CO<sub>2</sub> that is equivalent to 1 ppm of CO<sub>2</sub> in the atmosphere by volume, E is CO<sub>2</sub> emissions in million metric tons, and, N is the year. The results of the calculations [see Supplementary Material] are shown in Figure 4.

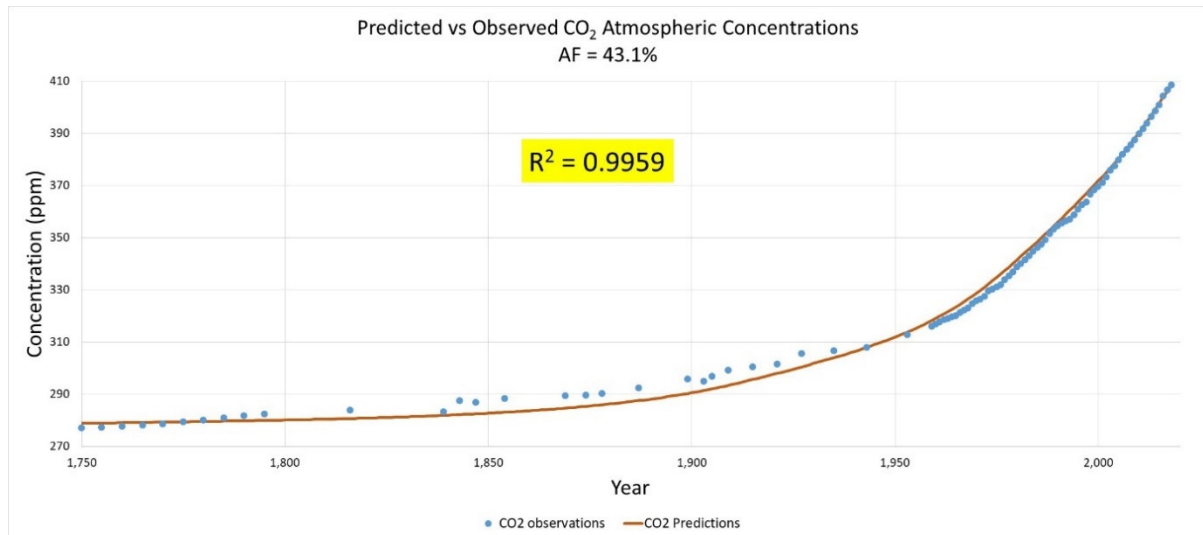


**Figure 4.** Comparison of predicted CO<sub>2</sub> concentrations with observations. Curve is best fit to data using Equation (1) with  $\alpha_1 = AF = 43.1\%$ .

The fitted curve based on Equation (1) shows that the predicted concentrations follow the CO<sub>2</sub> concentration observations reasonably well but are not a precise match. To examine this further, it is illustrative to examine the CO<sub>2</sub> emissions more closely as a function of time to determine if an exponential growth curve assumption for emissions is warranted and hence, implying a constant value for AF. Figure 1(b) shows the land-use CO<sub>2</sub> emissions [9,10]. A cursory examination of these data clearly demonstrates that the emissions do not follow an exponential growth pattern.

Now, consider fossil-fuel-based emissions in the time period from 1751 to 2018 [7,8], shown in Figure 5(a). As may be seen, the agreement between the best fit exponential growth curve with the data is poor in the early 20th century and significantly worse post-1980. Although the data from the nineteenth century (Figure 5(b)) clearly follow an exponential growth curve (note the logarithmic scale in Figure 5(b)), the data post-1945 are best fit by a linear growth curve (Figure 5(c)).

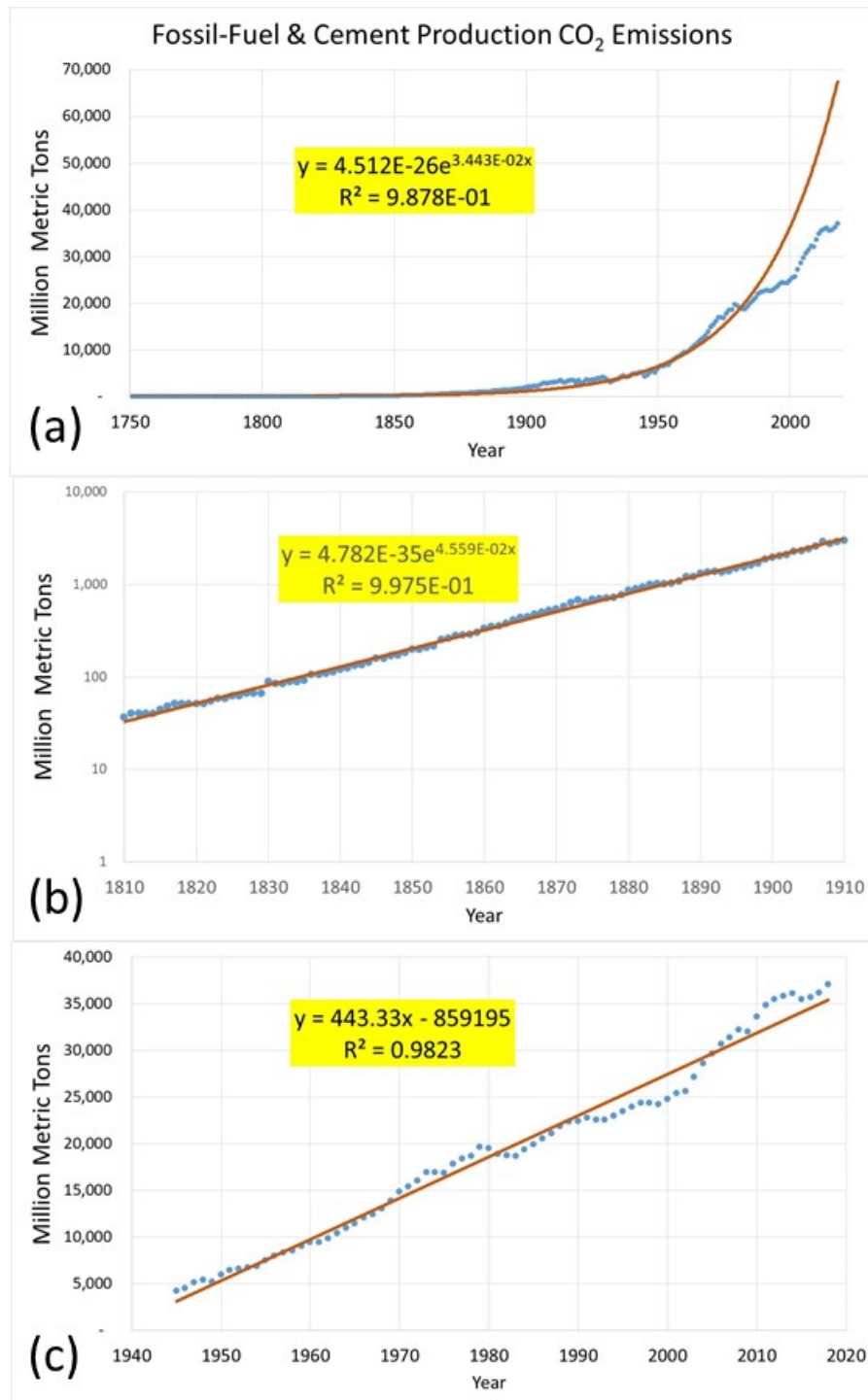


**Figure 5.** (a) Comparison of best fit exponential growth curve with fossil fuel and cement production CO<sub>2</sub> emissions (1750–2018). (b) Comparison of best fit exponential growth curve with fossil fuel and cement production CO<sub>2</sub> emissions (1810–1910). (c) Comparison of best fit linear growth curve with fossil fuel and cement production CO<sub>2</sub> emissions (1945–2018).

Although there is moderate agreement between the CO<sub>2</sub> concentration observations with those predicted by Equation (1) with a fixed value of 43.1% for AF, the deviations from exponential growth of both the carbon emissions from land-use changes (Figure 1(b)) and from fossil fuels (Figure 5(a) and (c)) suggest that the approximate concurrence observed in Figure 3 of the sum of the emissions with an exponential growth curve is coincidental and not indicative of a fundamental physical nature of the emissions. This issue raises concerns with the postulate [31] that if the climate system is

considered as a linear system forced by exponentially growing CO<sub>2</sub> emissions, then all the ratios of responses to forcings, including AF, are constant.

It is also illustrative to consider that from 1750 to 1850, the total CO<sub>2</sub> emissions [fossil fuel (FF) + land-use change (LUC)] equaled 71.7 Gt CO<sub>2</sub> with 93.4% of those emissions due to land-use changes [7,8,10]. Using the conversion factor of 1 ppm of CO<sub>2</sub> in the atmosphere by volume is equivalent to 7.782 Gtons CO<sub>2</sub> [9], this equates to a 9.2 ppm increase of CO<sub>2</sub> in the atmosphere if all the emitted CO<sub>2</sub> remained in the atmosphere. The measured data [15,16] indicate a 9.8 ppm increase in CO<sub>2</sub> atmospheric concentrations during that period. So, for 100 years at the beginning of the industrial era, this concurrence implies that ~100% of the total CO<sub>2</sub> emissions remained in the atmosphere. This somewhat surprising result raises the question: why is there apparently no evidence of an ocean or land-based carbon sink during this century-long time span?

### 3.1.2. Alternative Correlation Approach

In the same manner as used to generate Figure 4, a measured base-year [2018] concentration datum of 408.52 ppm was chosen from the Mauna Loa CO<sub>2</sub> measurements data set [17,18]. The change in the atmospheric CO<sub>2</sub> concentration was then determined by using only the fossil-fuel-based CO<sub>2</sub> emissions [7,8] for each year preceding 2018, converting those annual emission rates into an equivalent ppm of the atmosphere, and then applying a single scaling factor (AF<sub>FF</sub>) for each year to determine the concentration change for that year. For each year prior to 2018, the change was negative. Using Equation (1), the best fit curve to the data yields  $\alpha_2 = \text{AF}_{\text{FF}} = 54.5\%$ . The results of the calculations [see Supplementary Material] are shown in Figure 6.

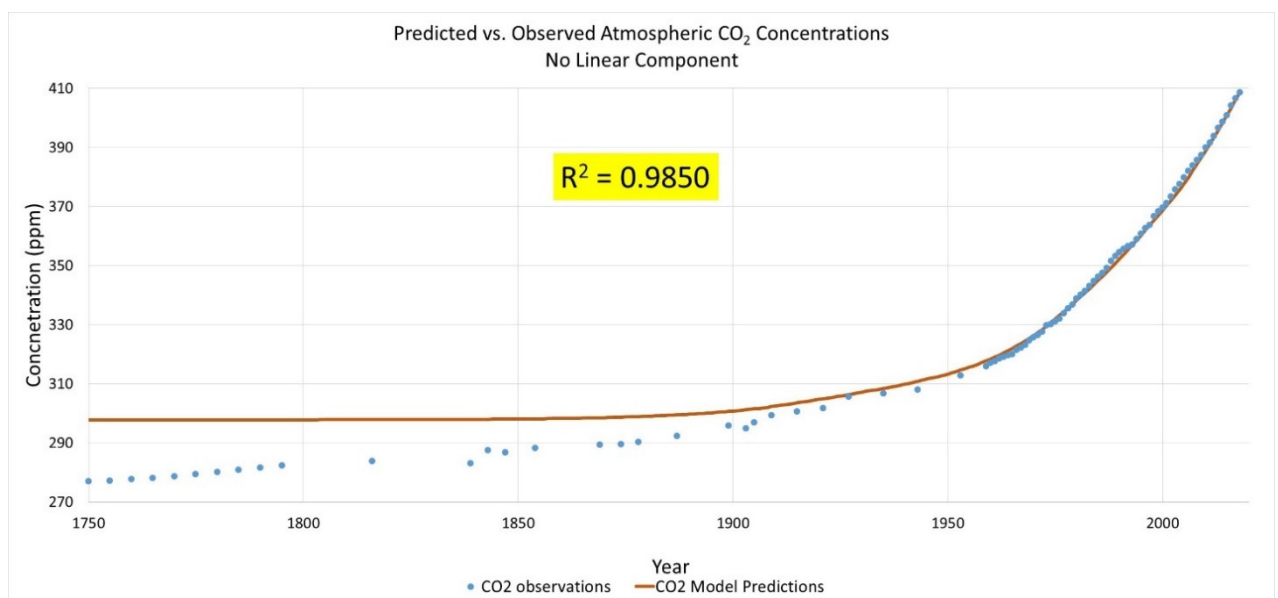


**Figure 6.** Measured and predicted CO<sub>2</sub> concentrations based on a 2018 datum base year. Curve is best fit to data using Equation (1) with scaling factor  $\alpha_2 = 54.5\%$  (AF<sub>FF</sub>).

There is excellent agreement between the predicted values and experimental observations from approximately 1925 to 2018. The agreement before 1925 is less precise because the predicted values become asymptotic as the CO<sub>2</sub> emissions from fossil fuel combustion and cement production diminish significantly during the nineteenth and eighteenth centuries while the measured atmospheric CO<sub>2</sub> concentration values from the Siple [16] and Law Dome [15] ice cores continue a steady decline as one moves backward in time from about 1925 to 1750.

To further refine the correlation of emissions with concentration, a closer examination of the measured CO<sub>2</sub> concentration data from 1750 to 1890 was performed. As may be seen in Figure 7, the increase in the non-fossil fuel/cement production-driven CO<sub>2</sub> atmospheric concentration over the 140-



year period is well characterized by a simple linear function. [The 1839 data point (brown triangle) was deselected from the analysis because the datum was considered out of range as its deviation from the best fit linear function was greater than 3X that of any other data point in the 1750–1890 data set.]

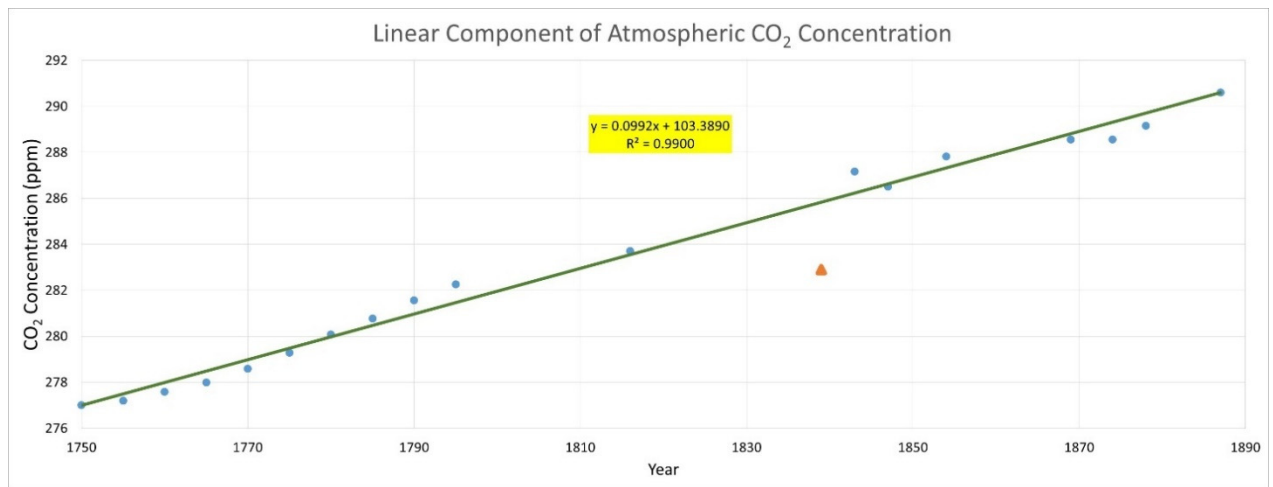


**Figure 7.** Atmospheric CO<sub>2</sub> concentrations with no fossil fuel combustion/cement production emissions inputs (Note: 1839 data point removed from analysis).

One may now characterize the overall change in atmospheric CO<sub>2</sub> concentration since 1750 as a superposition of the linear increase shown in Figure 7 extended through the present combined with the delta induced by fossil fuel/cement production-driven CO<sub>2</sub> emissions using an approach similar to that employed in Figure 6. The governing equation is:

$$ATM_{N-1} = ATM_N - (\alpha_i/\beta) \times E_{N-1} \times 10^9 - \kappa \tag{2}$$

where ATM is an atmospheric concentration in ppm,  $\alpha_i$  is  $AF_{FF}$  [ $\alpha_3$  determined by best fit to be 51.3%],  $\beta = 7.782Pg$  of CO<sub>2</sub> that is equivalent to 1 ppm of CO<sub>2</sub> in the atmosphere by volume,  $\kappa = 0.0992$  is the slope of the linear component of atmospheric CO<sub>2</sub> concentration (see Figure 7), E is fossil fuel combustion CO<sub>2</sub> emissions in million metric tons, and N is the year. The resultant agreement to the measured data is shown in Figure 8 [see Supplementary Material].

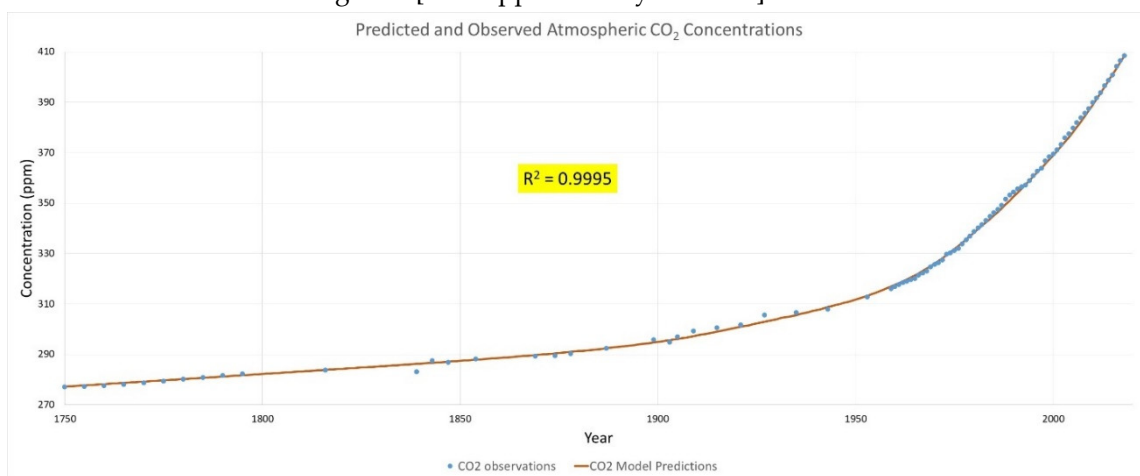


**Figure 8.** Measured and predicted CO<sub>2</sub> concentrations based on a 2018 datum base year. Curve is best fit to data using Equation (2) with scaling factor  $\alpha_3 = 51.3\%$  ( $AF_{FF}$ ).



An analysis of the statistical validity of the fit of the semi-empirical model [Equation (2)] to the measured data was performed [see Supplementary Material] using Anova in Microsoft Excel [35]. A linear regression of the predicted atmospheric CO<sub>2</sub> values versus the measured CO<sub>2</sub> levels yields the results shown in Figure 9. The slope of 1.008 (R-square: 0.9995) demonstrates almost a perfect fit with a robust statistically significant relationship (p-value: 3.2E-140). This result provides strong statistical evidence that A<sub>FF</sub> has been unchanged at 51.3 ± 0.4% (95% confidence interval) for the entire analysis period of 268 years.

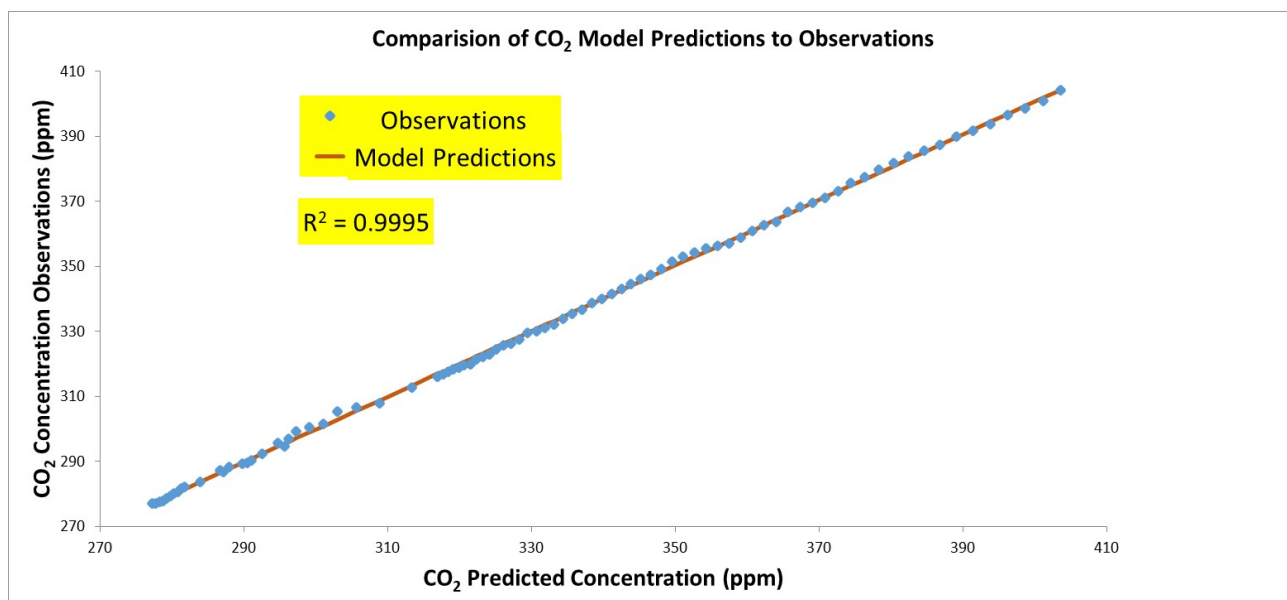


Figure 9. Comparison of predicted CO<sub>2</sub> atmospheric concentrations to observations.

#### 4. Discussion

Using the terminology of Le Quéré et al. [9], the global carbon budget is a balance of emission and absorption processes. This balance equation may be written as:

$$G_{ATM} = E_{FF} + E_{LUC} - S_{OCEAN} - S_{LAND} + B_{IM} \quad (3)$$

where  $G_{ATM}$  is the growth rate of CO<sub>2</sub> in the atmosphere;  $E_{FF}$  is the estimate for CO<sub>2</sub> emissions from fossil fuel combustion and cement production;  $E_{LUC}$  is the estimate for CO<sub>2</sub> emissions resulting from deliberate human activities on land;  $S_{OCEAN}$  is the uptake of CO<sub>2</sub> in the ocean;  $S_{LAND}$  is the uptake of CO<sub>2</sub> by the terrestrial sink; and,  $B_{IM}$  is an estimate of the budget imbalance, which is a measure of the mismatch between the estimated emissions and the estimated changes in the atmosphere, land, and ocean.

Referring to Figure 1(a), one observes significant increases in fossil-fuel combustion and cement production CO<sub>2</sub> emissions,  $E_{FF}$ , since the mid-1700s and since 1959, emissions have increased 370% [7,8]. Models of the ocean sink,  $S_{OCEAN}$ , have also shown increases from 5.5 ± 1.8 GtCO<sub>2</sub> during the decade of the 1960s to 9.2 ± 1.8 GtCO<sub>2</sub> from 2000 to 2009 [9,20–22]. These emissions and ocean sink increases have generally varied smoothly over time (see Figure 3 of [9]).

$E_{LUC}$  has demonstrated significant interannual variability over the past two decades [9] while changes prior to 1990 have been depicted as slowly varying in the literature [9,10,32]. It is possible that the significant interannual changes since 1990 were present in  $E_{LUC}$  pre-1990 but the estimates of the data or the models smoothed out changes from year to year. The land sink,  $S_{LAND}$ , has also increased over the past six decades but there has been dramatic variability in CO<sub>2</sub> absorption over

short time periods estimated using either DGVMs [36–46] or using the residual from Equation (3) with inputs of measured and modeled  $E_{FF}$ ,  $E_{LUC}$ ,  $G_{ATM}$ , and  $S_{OCEAN}$  [9].

To account for the significant interannual variability in the land sink, it may be hypothesized that the terrestrial carbon sink is a combination of two elements; one component that is slowly varying,  $S_{LAND\ SMOOTH}$ , that responds to smooth changes in the emissions of  $CO_2$ , coupled with a reactive component,  $S_{LAND\ REACTIVE}$ , that responds to rapid changes in emissions and is likely correlated with the rapid changes in vegetation considered in DGVMs. This approach would enable the terrestrial sink to adapt to rapid changes in land-based emissions (and correlate with the significant variation in interannual terrestrial sink estimates) while also accounting for a fraction of the more smoothly varying fossil-fuel-based emissions.

As shown in Figure 8, it is possible to fully characterize the change in  $CO_2$  concentrations over a 268-year period using only one measured concentration datum [2018-Mauna Loa [17,18]] combined with a linear regression fit to land-use change induced  $CO_2$  concentration increases and a fixed-parameter scaled,  $A_{FF}$ , calculation of the changes in  $CO_2$  concentration due to fossil fuel combustion and cement production emissions prior to 2018. Based on these data, it is suggested that Equation (3) may be used to determine the net flux of land-based  $CO_2$  emissions,  $E_{LUC}$ , combined with the reactive component of the terrestrial sink,  $S_{LAND\ REACTIVE}$ , from 1750 AD to the present. As observed in Figure 7, the growth rate of  $G_{ATM}$  was constant during the selected time period, increasing approximately 0.099 ppm per year. Converting this increase to a net emissions rate, it is determined that the net flux of  $E_{LUC}$  minus  $S_{LAND\ REACTIVE}$  is 0.77 Gt $CO_2$  per year. The remainder of the land sink,  $S_{LAND\ SMOOTH}$ , coupled with the ocean sink operates as a smoothly varying function that absorbs 48.7% of the emissions from fossil fuels and cement production. This somewhat non-intuitive hypothesis of two constituents comprising the terrestrial sink is borne out by the data.

### Uncertainties

Each data set used in the analysis have uncertainties associated with the information. These include measurement uncertainty, uncertainty in the estimates of data, and uncertainties in the application of models to match physical measurements. For ice core data, sources of uncertainty include: timescale uncertainty that has been estimated to be  $\pm 2$  years for the data included in this analysis [15,16]; sampling uncertainty, spatial uncertainty as snowfall may vary significantly over short distance; diffusion uncertainty where the characteristic length of diffusion may exceed the characteristic depth resolution proxy used in the analysis; and, uncertainties with respect to the assumptions of the relationships between variables over time [47].

$E_{FF}$  uncertainties are impacted by the availability of accurate and complete records for each of the pertinent quantities that input into the total value of  $E_{FF}$ . When these are included, the total uncertainty has been estimated to range from 5% to 10% across the time range of the study [9,11–13].  $E_{LUC}$  uncertainties have been estimated to be more significant. For bookkeeping models, uncertainties range from 47% to 58% while for DGVMs they range from 32% to 50% [9].

The values for the terrestrial sink also have significant uncertainties. The residual sink uncertainties determined using Equation (3) range from 29% to 60% of the estimated  $S_{LAND}$  values [9]. Approaches using DGVMs have uncertainties that range from 19% to 41% depending upon the selected time frame [9]. The ocean sink uncertainties range from 20% to 50% depending upon the selected decade under study. The inclusion of these uncertainties into the fitting may impact the reliability of the model to determine  $CO_2$  concentration values based on  $E_{FF}$  and  $E_{LUC}$ . In particular, the uncertainties noted in  $E_{LUC}$  over the past six decades [9] imply that for a number of decades, there may have been zero emissions due to land-use change. These would call into question the validity of the linear component determined from the best fit of  $E_{LUC}$  values that is shown in Figure 7 and hence the validity of the postulate to separate the terrestrial carbon sink into two elements. Additional research is suggested to resolve this potential issue.

## 5. Conclusions

A semi-empirical model has been developed to calculate CO<sub>2</sub> concentrations from 1751 to 2018 as a function of CO<sub>2</sub> emissions. Initial calculations using only E<sub>FF</sub> data and a constant value of A<sub>FF</sub> = 54.5% enabled excellent replication of concentration observations from 1925 to 2018 but prior to 1925, the agreement was less precise. Predicted values become asymptotic as the E<sub>FF</sub> levels diminish significantly during the nineteenth and eighteenth centuries while the measured atmospheric CO<sub>2</sub> concentration values continue a steady decline as one moves backward in time from about 1925 to 1750. To improve the agreement between the predicted and measured CO<sub>2</sub> concentration values, the relationship between concentration and emissions was postulated to be a superposition of two elements. The first element with a constant concentration growth rate for the time period under consideration may be attributed to the net flux of land-use changes with a rapidly varying reactive component of the terrestrial sink. The second element is determined by a calculation using fossil-fuel combustion emissions with a single, fixed factor, A<sub>FF</sub>, that has been determined to be unchanging over the period. It is postulated the value of A<sub>FF</sub> is determined by a combination of the ocean sink with a smoothly varying component of the terrestrial sink. The agreement between predicted and observed CO<sub>2</sub> concentrations is excellent across the considered time period and has determined to a strong statistical validity that A<sub>FF</sub> has been unvarying at 51.3% for the past 268 years. If one considers the changes in factors such as emission and sequestration processes (see, e.g., Figure 1.1 from the IPCC AR5 report [32]) coupled with the non-exponential growth patterns of land-based or fossil-fuel-driven emissions negating the eigenvector approach of [31], a constant A<sub>FF</sub> applied as in Equation (2) to fossil-fuel CO<sub>2</sub> emissions [7,8] to accurately reproduce the changes in CO<sub>2</sub> concentrations may be judged significant and worthy of additional study.

**Supplementary Materials:** The following are available online at [www.mdpi.com/2225-1154/8/5/61/s1](http://www.mdpi.com/2225-1154/8/5/61/s1). The datasets generated and/or analyzed during the current study have been included with the Supplementary Materials attached to this manuscript.

**Funding:** This research received no external funding.

**Conflicts of Interest:** The author declares no conflict of interest.

## References

1. Fleming, J.R. *Historical Perspectives on Climate Change*; Oxford University Press: Oxford, UK, 1998.
2. Tyndall, J. On the Absorption and Radiation of Heat by Gases and Vapours, and on the Physical Connexion of Radiation, Absorption, and Conduction. *Phil. Trans. R. Soc.* **1861** 151, 1–36.
3. Oreskes, N. The scientific consensus on global warming. *Science* **2004**, *306*, 1686.
4. Prentice, I.C.; Farquhar, G.D.; Fasham, M.J.R.; Goulden, M.L.; Heimann, M.; Jaramillo, V.J.; Kheshgi, H.S.; LeQuéré, C.; Scholes, R.J.; Wallace, D.W.R.; et al. *Climate Change 2001: The Scientific Basis. Contributions of Working Group I to the Third Assessment Report of the Intergovernmental Panel on Climate Change*; Cambridge University Press: Cambridge, UK, 2001; pp. 185–237.
5. Meehl, G.A.; Covey, C.; Delworth, T.; Latif, M.; McAvaney, B.; Mitchell, J.F.B.; Stouffer, R.J.; Taylor, K.E. THE WCRP CMIP3 MULTIMODEL DATASET A New Era in Climate Change Research. *BAMS* **2007**, 1383–1394, doi:10.1175/BAMS-88-9-1383.
6. Andres, R.J.; Boden, T.A.; Bréon, F.-M.; Ciais, P.; Davis, S.; Erickson, D.; Gregg, J.S.; Jacobson, A.; Marland, G.; Miller, J.; et al. A synthesis of carbon dioxide emissions from fossil-fuel combustion. *Biogiosciences* **2012**, *9*, 1845–1871, doi:10.5194/bg-9-1845-2012.
7. Boden, T.A.; Andres, R.J.; Marland, G. *Global, Regional, and National Fossil-Fuel CO<sub>2</sub> Emissions*; Carbon Dioxide Information Analysis Center, Oak Ridge National Laboratory, U.S. Department of Energy: Oak Ridge, TN, USA, 2013. Available online: [http://cdiac.ess-dive.lbl.gov/trends/emis/overview\\_2010.html](http://cdiac.ess-dive.lbl.gov/trends/emis/overview_2010.html) (accessed on 20 January 2020).
8. Boden, T.A.; Marland, G.; Andres, R.J. *Global, Regional, and National Fossil-Fuel CO<sub>2</sub> Emissions*; Carbon Dioxide Information Analysis Center at Appalachian State University: Boone, NC, USA, 2018. Available online: <https://energy.appstate.edu/CDIAC> (accessed on 20 January 2020).

9. Le Quéré, C.; Robbie, A.M.; Friedlingstein, P.; Sitch, S.; Hauck, J.; Pongratz, J.; Pickers, P.A.; Korsbakken, J.I.; Peters, G.P.; Canadell, J.G.; et al. Global Carbon Budget 2018. *Earth Syst. Sci. Data* **2018**, *10*, 2141–2194, doi:10.5194/essd-10-2141-2018.
10. Stocker, B.D.; Feissli, F.; Strassmann, K.M.; Spahni, R.; Joos, F. Past and future carbon fluxes from land use change, shifting cultivation and wood harvest. *Tellus B Chem. Phys. Meteorol.* **2014**, *66*, 23188, doi:10.3402/tellusb.v66.23188.
11. Andres, R.J.; Fielding, D.J.; Marland, G.; Boden, T.A.; Kumar, N.; Kearney, A.T. Carbon dioxide emissions from fossil-fuel use, 1751–1950. *Tellus B* **1999**, *51*, 759–765.
12. Andres, R.J.; Boden, T.; Higdon, D. A new evaluation of the uncertainty associated with CDIAC estimates of fossil fuel carbon dioxide emission. *Tellus B* **2014**, *66*, 23616, doi:10.3402/tellusb.v66.23616.
13. Ballantyne, A.P.; Andres, R.; Houghton, R.; Stocker, B.D.; Wanninkhof, R.; Anderegg, W.; Cooper, L.A.; DeGrandpre, M.; Tans, P.P.; Miller, J.B.; et al. Audit of the global carbon budget: Estimate errors and their impact on uptake uncertainty. *Biogeosciences* **2015**, *12*, 2565–2584, doi:10.5194/bg-12-2565-2015.
14. Hurtt, G.C.; Frolking, S.; Fearon, M.G.; Moore, B.; Shevliakova, E.; Malshev, S.; Pacala, S.W.; Houghton, R.A. The underpinnings of land-use history: Three centuries of global gridded land-use transitions, wood harvest activity, and resulting secondary landscapes. *Glob. Chan. Biol.* **2006**, *12*, 1208–1229, doi:10.1111/j.1365-2486.2006.01150.x.
15. Etheridge, D.M.; Steele, L.P.; Langenfelds, R.L.; Francey, R.J.; Barnola, J.-M.; Morgan, V.I. *Historical CO<sub>2</sub> Records from the Law Dome DE08, DE08-2, and DSS ice cores In Trends: A Compendium of Data on Global Change*; Carbon Dioxide Information Analysis Center, Oak Ridge National Laboratory, U.S. Department of Energy: Oak Ridge, TN, USA, 1998. Available online: <http://cdiac.ess-dive.lbl.gov/trends/co2/lawdome.html> (accessed on 18 December 2019).
16. Neftel, A.; Friedli, H.; Moor, E.; Lötscher, H.; Oeschger, H.; Siegenthaler, U.; Stauffer, B. *Historical Carbon Dioxide Record from the Siple Station Ice Core in Trends: A Compendium of Data on Global Change*; Carbon Dioxide Information Analysis Center, Oak Ridge National Laboratory, U.S. Department of Energy: Oak Ridge, TN, USA, 1994. Available online: [Cdiac.ess-dive.lbl.gov/trends/co2/siple.html](http://cdiac.ess-dive.lbl.gov/trends/co2/siple.html) (accessed on 18 December 2019).
17. Tans, P. 2018. Available online: <http://www.esrl.noaa.gov/gmd/ccgg/trends/> (accessed on 18 December 2019).
18. Keeling, R.F. 2018. Available online: [scrippsco2.ucsd.edu](http://scrippsco2.ucsd.edu) (accessed on 18 December 2019).
19. Tans, P.; Thoning, K. “How we measure background CO<sub>2</sub> levels on Mauna Loa” NOAA ESRL Global Monitoring Division. 2018. Available online: [www.esrl.noaa.gov/gmd/ccgg/about/co2\\_measurements.html](http://www.esrl.noaa.gov/gmd/ccgg/about/co2_measurements.html) (accessed on 5 January 2020).
20. Wanninkhof, R.; Park, G.-H.; Takahasi, T.; Sweeney, C.; Reely, R.; Nojiri, Y.; Gruber, N.; Doney, S.C.; McKinley, G.A.; Lenton, A.; et al. Global ocean carbon uptake: Magnitude, variability and trends. *Biogeosciences* **2013**, *10*, 1983–2000, doi:10.5194/bg-10-1983-2013.
21. Plattner, G.-K.; Joos, F.; Stocker, T.F.; Marchal, O. Feedback mechanisms and sensitivities of ocean carbon uptake under global warming. *Tellus B Chem. Phys. Meteorol.* **2001**, *53*, 564–592, doi:10.3402/tellusb.v53i5.16637.
22. Khatiwala, S.; Primeau, F.; Hall, T. Reconstruction of the history of anthropogenic CO<sub>2</sub> concentrations in the ocean. *Nature* **2009**, *462*, 346–349, doi:10.1038/nature08526.
23. Boysen, L.R.; Brovkin, V.; Arora, V.K.; Cadule, P.; de Noblet-Ducoudré, N.; Kato, E.; Pongratz, J.; Gayler, V. Global and regional effects of land-use change on climate in 21st century simulations with interactive carbon cycle. *Earth Syst. Dyn.* **2014**, *5*, 309–319.
24. Matthews, H.; Weaver, A.; Meissner, K.; Gillett, N.; Eby, M. Natural and anthropogenic climate change: Incorporating historical land cover change, vegetation dynamics and the global carbon cycle. *Clim. Dyn.* **2004**, *22*, 461–479.
25. Brovkin, V.; Sitch, S.; von Bloh, W.; Claussen, M.; Bauer, E.; Cramer, W. Role of land cover changes for atmospheric CO<sub>2</sub> increase and climate change during the last 150 years. *Glob. Change. Biol.* **2004**, *10*, 1253–1266.
26. Brovkin, V.; Boysen, L.; Arora, V.; Boisier, J.; Cadule, P.; Chini, L.; Claussen, M.; Friedlingstein, P.; Gayler, V.; van den Hurk, B.J.J.M.; et al. Effect of anthropogenic land-use and land cover changes on climate and land carbon storage in CMIP5 projections for the 21st century. *J. Clim.* **2013**, *26*, 6859–6881, doi:10.1175/JCLI-D-12-00623.1.

27. Sitch, S.; Brovkin, V.; von Bloh, W.; van Vuuren, D.; Eickhout, B.; Ganopolski, A. Impacts of future land cover changes on atmospheric CO<sub>2</sub> and climate. *Glob. Biogeochem. Cycles* **2005**, *19*, GB2013, doi:10.1029/2004GB002311.
28. Shevliakova, E.; Stouffer, R.J.; Malyshev, S.; Krasting, J.P.; Hurtt, G.C.; Pacala, S.W. Historical warming reduced due to enhance land carbon uptake. *Proc. Natl. Acad. Sci. USA* **2013**, *110*, 16730–16735.
29. Pongratz, J.; Reick, C.; Raddatz, T.; Claussen, M. Biogeophysical vs. biogeochemical climate response to historical anthropogenic land cover change. *Geophys. Res. Lett.* **2010**, *37*, L08072, doi:10.1029/2010GL043010.
30. Bennedsen, M.; Hillebrand, E.; Koopman, S.J. Trend analysis of the airborne fraction and sink rate of anthropogenically released CO<sub>2</sub>. *Biogeosciences* **2019**, *16*, 3651–3663.
31. Raupach, M.R.; Canadell, J.G.; LeQuéré, C. Anthropogenic and biophysical contributions to increasing atmospheric CO<sub>2</sub> growth rate and airborne fraction. *Biogeosciences* **2008**, *5*, 1601–1613.
32. Stocker, T.F.; Qin, D.; Plattner, G.-K.; Tignor, M.; Allen, S.K.; Boschung, J.; Nauels, A.; Xia, Y.; Bex, V.; Midgley, P.M. (Eds) *Climate Change 2013: The Physical Science Basis. Contribution of Working Group I to the Fifth Assessment Report of IPCC the Intergovernmental Panel on Climate Change*; Cambridge University Press: Cambridge, UK; New York, NY, USA, 2013.
33. Terenzi, F.; Khattiwala, S. Modeling the atmospheric airborne fraction in a simple carbon cycle model. *Tellus B* **2009**, submitted.
34. Trenberth, K.E.; Smith, L. The Mass of the Atmosphere: A Constraint on Global Analyses. *J. Clim.* **2005**, *18*, 864–875.
35. Microsoft Corporation. Microsoft Excel. 2018. Available online: <https://office.microsoft.com/excel> (accessed on 12 February 2020).
36. Lawrence, D.M.; Oleson, K.W.; Flanner, M.G.; Thornton, P.E.; Swenson, S.C.; Lawrence, P.J.; Zeng, X.; Yang, Z.-L.; Levis, S.; Sakaguchi, K.; et al. Parameterization improvements and functional and structural advances in version 4 of the Community Land Model. *J. Adv. Model. Earth Syst.* **2011**, *3*, M03001, doi:10.1029/2012MS000165.
37. Levy, P.E.; Cannell, M.G.R.; Friend, A.D. Modelling the impact of future changes in climate, CO<sub>2</sub> concentration and land use on natural ecosystems and the terrestrial carbon sink. *Glob. Environ. Chang.* **2004**, *14*, 21–30, doi:10.1016/j.gloenvcha.2003.10.005.
38. Clark, D.B.; Mercado, L.M.; Sitch, S.; Jones, C.D.; Gedney, N.; Best, M.J.; Pryor, M.; Rooney, G.G.; Essery, R.L.H.; Blyth, E.; et al. The Joint UK Land Environment Simulator (JULES), model description – Part 2: Carbon fluxes and vegetation dynamics. *Geosci. Model Dev.* **2011**, *4*, 701–722, doi:10.5194/gmd-4-701-2011.
39. Cox, P.M. Description of the “TRIFFID” Dynamic Global Vegetation Model; Hadley Centre: Exeter, UK, 2001. Technical Note 24 2001.
40. Sitch, S.; Smith, B.; Prentice, I.C.; Arneth, A.; Bondeau, A.; Cramer, W.; Kaplan, J.O.; Levis, S.; Lucht, W.; Sykes, M.T.; et al. Evaluation of ecosystem dynamics, plant geography and terrestrial carbon cycling in the LPJ dynamic global vegetation model. *Glob. Change. Biol.* **2003**, *9*, 161–185, doi:10.1046/j.1365-2486.2003.00569.x.
41. Smith, B.; Prentice, I.C.; Sykes, M.T. Representation of vegetation dynamics in the modelling of terrestrial ecosystems: Comparing two contrasting approaches within European climate space. *Glob. Ecol. Biogeogr.* **2001**, *10*, 621–637, doi:10.1046/j.1466-822X.2001.t01-1-00256.x.
42. Ahlström, A.; Miller, P.A.; Smith, B. Too early to infer a global NPP decline since 2000. *Geophys. Res. Lett.* **2012**, *39*, L15403, doi:10.1029/2012GL052336.
43. Zaehle, S.; Ciais, P.; Friend, A.D.; Prieur, V. Carbon benefits of anthropogenic reactive nitrogen offset by nitrous oxide emissions. *Nat. Geosci.* **2011**, *4*, 601–605, doi:10.1038/ngeo1207.
44. Krinner, G.; Viovy, N.; de Noblet-Ducoudré, N.; Ogee, J.; Polcher, J.; Friedlingstein, P.; Ciais, P.; Sitch, S.; Prentice, I.C. A dynamic global vegetation model for studies of the coupled atmosphere-biosphere system. *Glob. Biogeochem. Cycles* **2005**, *19*, Gb1015, doi:10.1029/2003gb002199.
45. Woodward, F.I.; Lomas, M.R. Vegetation dynamics—simulating responses to climatic change. *Biol. Rev.* **2004**, *79*, 643–670, doi:10.1017/s1464793103006419.
46. Zeng, N.; Mariotti, A.; Wetzell, P. Terrestrial mechanisms of interannual CO<sub>2</sub> variability. *Glob. Biogeochem. Cycles* **2005**, *19*, GB1016, doi:10.1029/2004gb002273.
47. Steig, E.J. Sources of Uncertainty in Ice Core Data. In *White paper from Workshop on Reducing and Representing Uncertainties in High-Resolution Proxy Data*; PAGES/CLIVAR Proxy Uncertainty Workshop: Trieste, Italy 2008.



© 2020 by the author. Licensee MDPI, Basel, Switzerland. This article is an open access article distributed under the terms and conditions of the Creative Commons Attribution (CC BY) license (<http://creativecommons.org/licenses/by/4.0/>).